Table S1. Clinical data of patients with aortic dissection and control cases.

	AD (*n*=108)	Control group (*n*=30)	*P* value
Age, Yrs*	55.63±11.63	53.23±9.40	0.30
Male (%)	81 (75.00%)	18 (60.00%)	0.38
Stanford Classification (%)			
Type A	75 (69.44%)	NA	NC
Type B	33 (30.56%)	NA	NC
BMI	26.95±4.59	26.11±2.70	0.21
Hypertension (%)	74 (68.52%)	6 (20.00%)	<0.001
Diabetes (%)	5 (4.63%)	3 (10.00%)	0.37
Coronary heart disease (%)	7 (6.48%)	0	0.35
Renal failure (%)	2 (1.85%)	0	>0.99
Atherosclerosis (%)	72 (66.67%)	3 (10.00%)	<0.001
Smoking history (%)	33 (30.56%)	1 (3.33%)	0.001
Poor distal organ perfusion (%)	17 (15.74%)	NA	NC
Time of onset (hours)	11.56±18.29	NA	NC
Maximum diameter of aorta (mm)*	43.95±8.11	NA	NC
Maximum diameter of false lumen (mm)*	23.16±9.45	NA	NC

Note, *present as mean ± SD; NA, not applicable; NC, not computable. For the analysis of binary categorical variables, we employed the Chi-square test to assess the association between groups. For continuous variables, we utilized the Wilcoxon rank-sum test to compare differences between the two groups, as it is appropriate for non-normally distributed data.

Table S2. Comparison of general characteristics between patients with aortic dissection and healthy control

	AD (*n*=20)	Control (*n*=10)	*P* value
Age, Yrs*	55.70±10.48	49.20±8.78	0.10
Gender			
Male	13 (65.00%)	9 (90.00%)	
Female	7 (35.00%)	1 (10.00%)	0.21
BMI*	26.13±2.87	25.77±3.42	0.76
Hypertension (%)	14 (65.00%)	7 (70.00%)	>0.99
Atherosclerosis (%)	13 (65.00%)	3 (30.00%)	0.12
Onset time (h)*	16.10±24.03	NA	NC

Note, *present as mean ± SD; NA, not applicable; NC, not computable. For the analysis of binary categorical variables, we employed the Chi-square test to assess the association between groups. For continuous variables, we utilized the Wilcoxon rank-sum test to compare differences between the two groups, as it is appropriate for non-normally distributed data.

Table S3. Clinical data of patients with aortic dissection and control case for scRNA-seq.

Characteristics	Normal aortic tissue	Aortic dissection tissue No. 1	Aortic dissection tissue No. 2
Gender	Male	Female	Male
Age	44	64	55
Diagnosis	Organ donor	Aortic dissection	Aortic dissection
History of hypertension	No	Yes	Yes
History of diabetes	No	No	No
Coronary artery disease	No	Yes	No
Aortic valve regurgitation	No	Yes	Yes
Bicuspid aortic valve	No	No	No
Atherosclerosis	No	Yes	No
Immune-related diseases	No	No	No
Immune-related diseases	Yes	Yes	No
Time from onset to sample collection (hours)	-	15	11

15

16 **Table S4**. mRNA primer sequence for human and mice

Gene (Species)	Forward	Reverse
SPHK1 (Human)	AAGACCTCCTGACCAACTGC	GGCTGAGCACAGAGAAGAGG
IL-1β(Human)	CCACAGACCTTCCAGGAGAAT	GTGCAGTTCAGTGATCGTACAG
IL-6 (Human)	AGTGAGGAACAAGCCAGAGC	CATTTGTGGTTGGGTCAGG
MMP2 (Human)	CCCACTGCGGTTTTCTCGAAT	CAAAGGGGTATCCATCGCCAT
MMP9 (Human)	TCGTGGTTCCAACTCGGTTT	GGTTTCCCATCAGCATTGCC
S1PR1 (Human)	GCTGGGTCATCTCCCTCAT	GCAGTTCCAGCCCATGAT
S1PR2 (Human)	CCAACAAGGTCCAGGAACAC	GCAACAGAGGATGACGATGA
S1PR3 (Human)	TCAGGGAGGGCAGTATGTTC	CCAGTAAGCTGCAGGTGGA
S1PR4 (Human)	GGCACAGCCGGCTCATTGTT	AAGCTGAGCACGGCTCTGCACA
S1PR5 (Human)	GTGAGGTGGGAGCCATAGAA	TCTAGAATCCACGGGGTCTG
β-actin (Human)	GGACTTCGAGCAAGAGATGG	AGCACTGTGTTGGCGTACAG
Sphk1 (Mouse)	CAAGTGCACCCAAACTACC	GCCCCACCTTCTAGCTTTCT
Mmp2 (Mouse)	CCCTCAAGAAGATGCAGAAGT	TCTTGGCTTCCGCATGGT
Mmp9 (Mouse)	CGTGTCTGGATTCGACTTGA	TTGGAAACTCACACGCCAGA
Il-1β (Mouse)	TGCCACCTTTTGACAGTGATG	TGTGCTGCTGCGAGATTTG
Il-6 (Mouse)	TCCAGTTGCCTTCTTGGGACT	TAAGCCTCCGACTTGTGAAGTG
S1p2 (Mouse)	ATAGACCGAGCACAGCCAAC	GAGGTGGTCTCCTGCATGTC
S1p3 (Mouse)	AAGCCTAGCGGGAGAGAAAC	TCAGGGAACAATTGGGAGAG
Sphk2 (Mouse)	CGGATGCCCATTGGTGTCCTC	TGAGCAACAGGTCAACACCGAC
Sgpp1(Mouse)	GCTTGTACTGTTCGTGAGGGA	GAACCCAACCATCCCGTAGG
Sgpp2 (Mouse)	TTCACCCACTGGAATATCGACC	AAGTCTCACAACGGGAGGAAA
Sgpl1 (Mouse)	TTTCCTCATGGTGTGATGGA	CCCCAGACAAGCATCCAC
Hif-1α(Mouse)	CATCATCTCTCTGGATTTTG	GAAGAGGGAAACATTACATC
Hk2 (Mouse)	TGATCGCCTGCTTATTCACGG	AACCGCCTAGAAATCTCCAGA
Pfkfb3 (Mouse)	TCATCGAGTCGGTCTGTGACG	CATGGCTTCTGCTGAGTTGCAG
β-actin (Mouse)	AGTGTGACGTTGACATCCGT	GCAGCTCAGTAACAGTCCGC

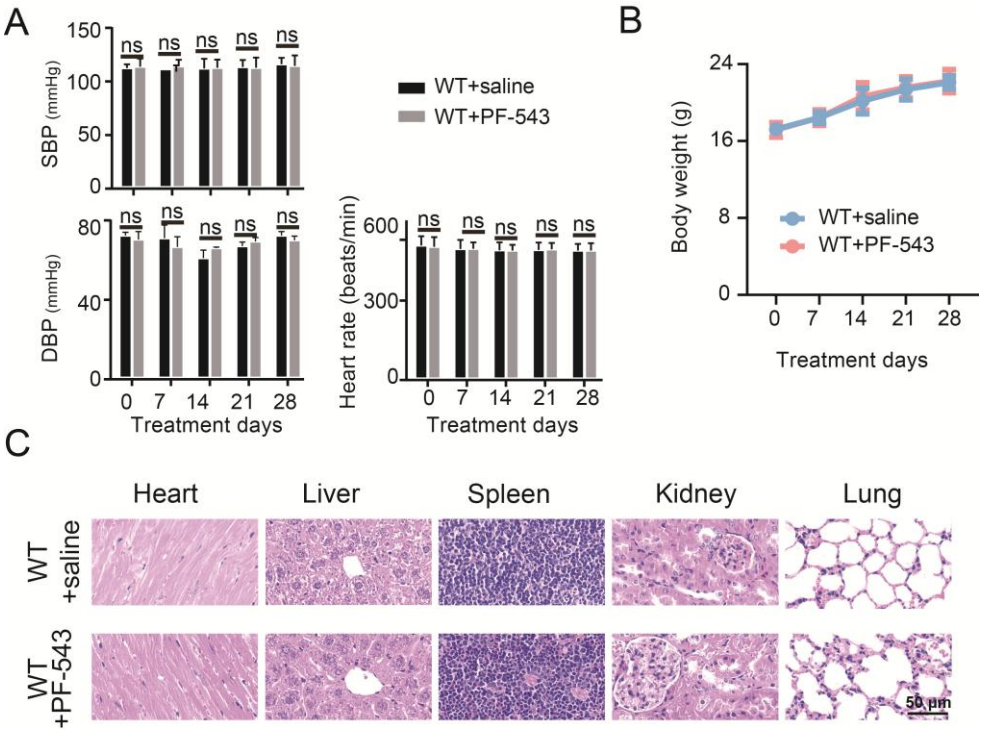

Figure S1. Potential toxicity assessment of PF-543. (A) Systolic and diastolic blood pressures, heart rates are measured in mice. Unpaired Student's *t*-test, ns, no significant. **(B)** Body weight changes in mice. **(C)** Histopathological studies *in vivo*. (A-B) n=3 per group. WT, wild-type.

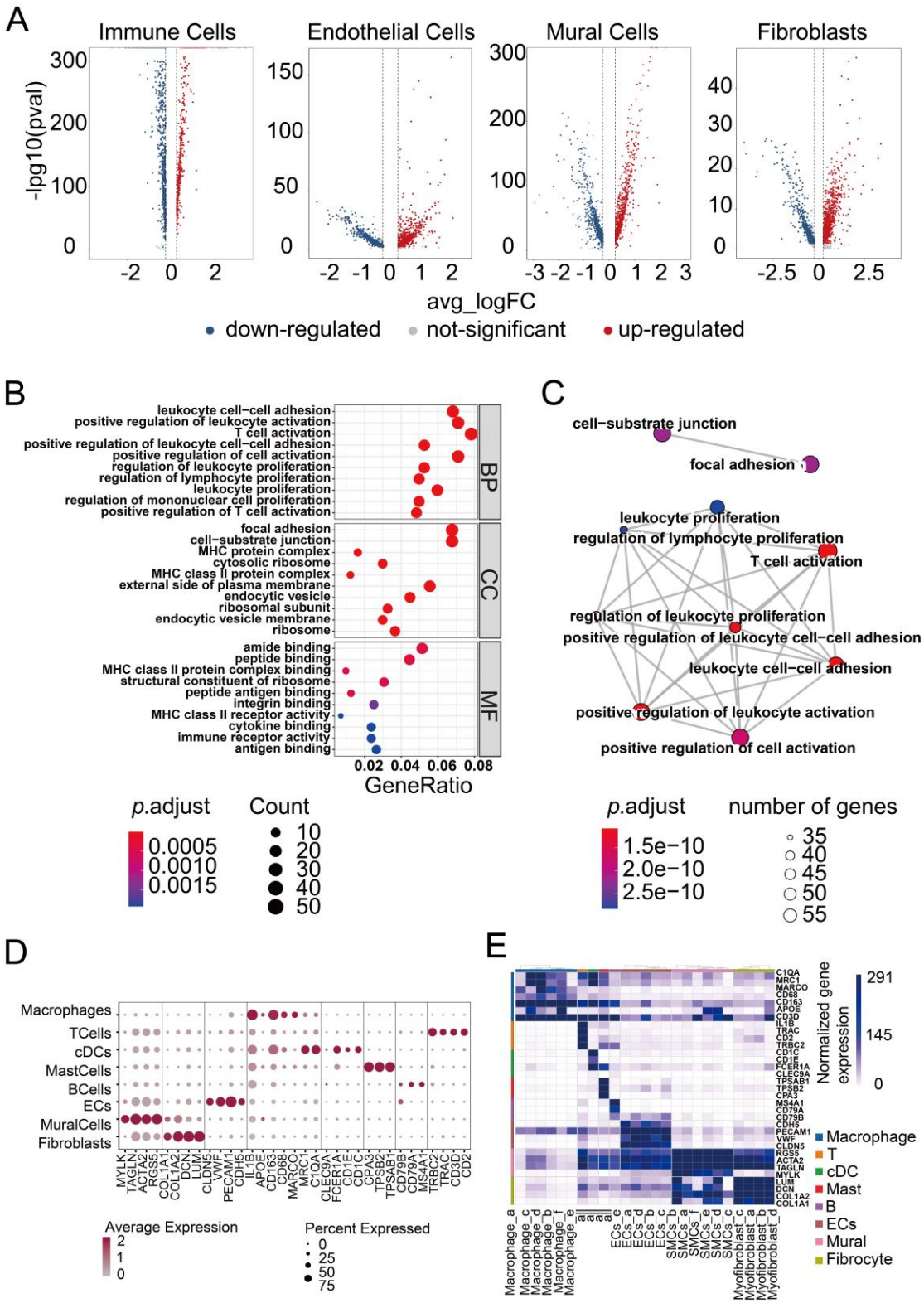

Figure S2. Differential gene expressions across cell subtypes and immune cell-enriched pathways. (A) The volcano plot illustrates the differentially expressed genes between each cell type and other cells, upregulated genes in red, downregulated

genes in blue, using the Wilcoxon rank-sum test to compare differences between groups). **(B)** Bubble chart for Gene Ontology (GO) enrichment analysis. The x-axis represents the enrichment factor, the y-axis indicates the signaling pathways, bubble size denotes the number of genes, and the color represents the adjusted *P*-value. **(C)** Network diagram illustrating the interactions between GO enrichment signals. **(D)** The bubble plot shows the expression of marker genes for each cell type, where the size of the circle represents the proportion of cells expressing the marker gene, and the color intensity represents the expression level. **(E)** Expression levels of marker genes in each cell subcluster.

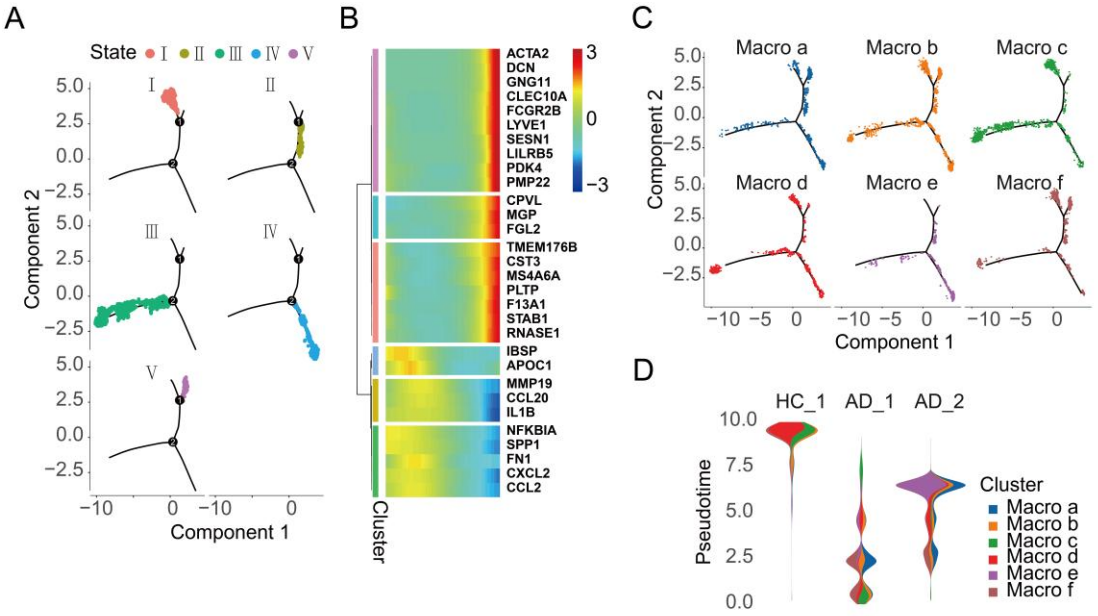

Figure S3. Macrophage trajectories and pseudotime analysis in aortic dissection (*n*=2). **(A)** Macrophage trajectories can be classified into cell states I-V. **(B)** Based on the inferred pseudotime, the heatmap shows the expression level changes of each gene. **(C)** The cell trajectories of each macrophage subcluster. **(D)** The pseudotime distribution of normal (*n*=1) and AD samples (*n*=2).

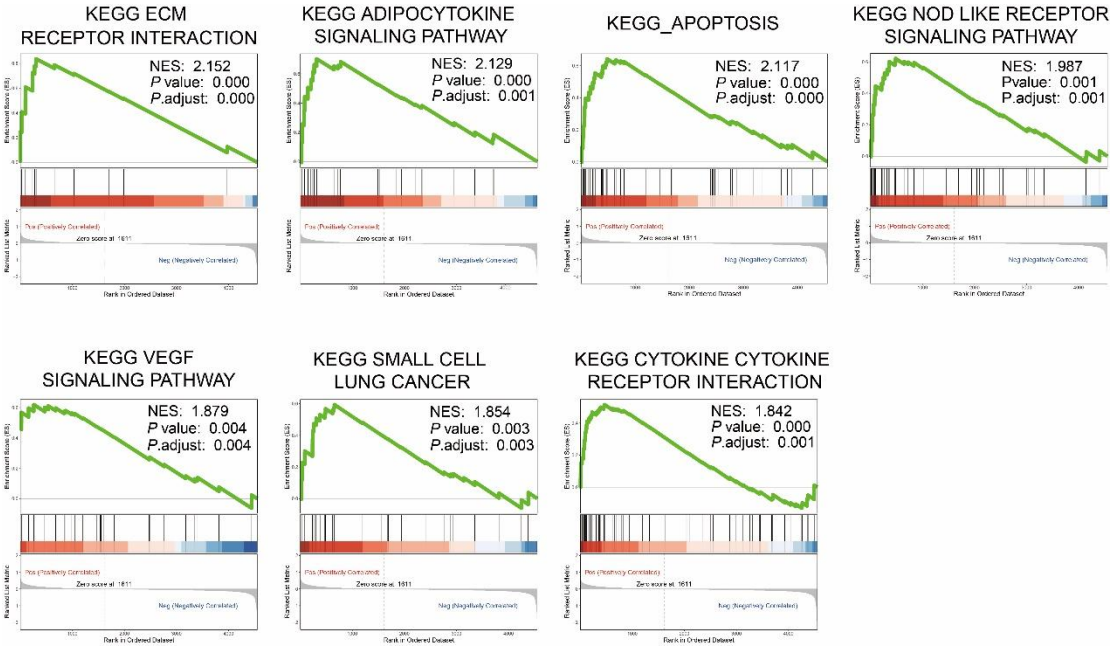

Figure S4. Single gene GSEA analysis of SPHK1 enrichment pathway in AD macrophage subcluster a. NES, Normalized Enrichment Score; GSEA, gene set enrichment analysis.

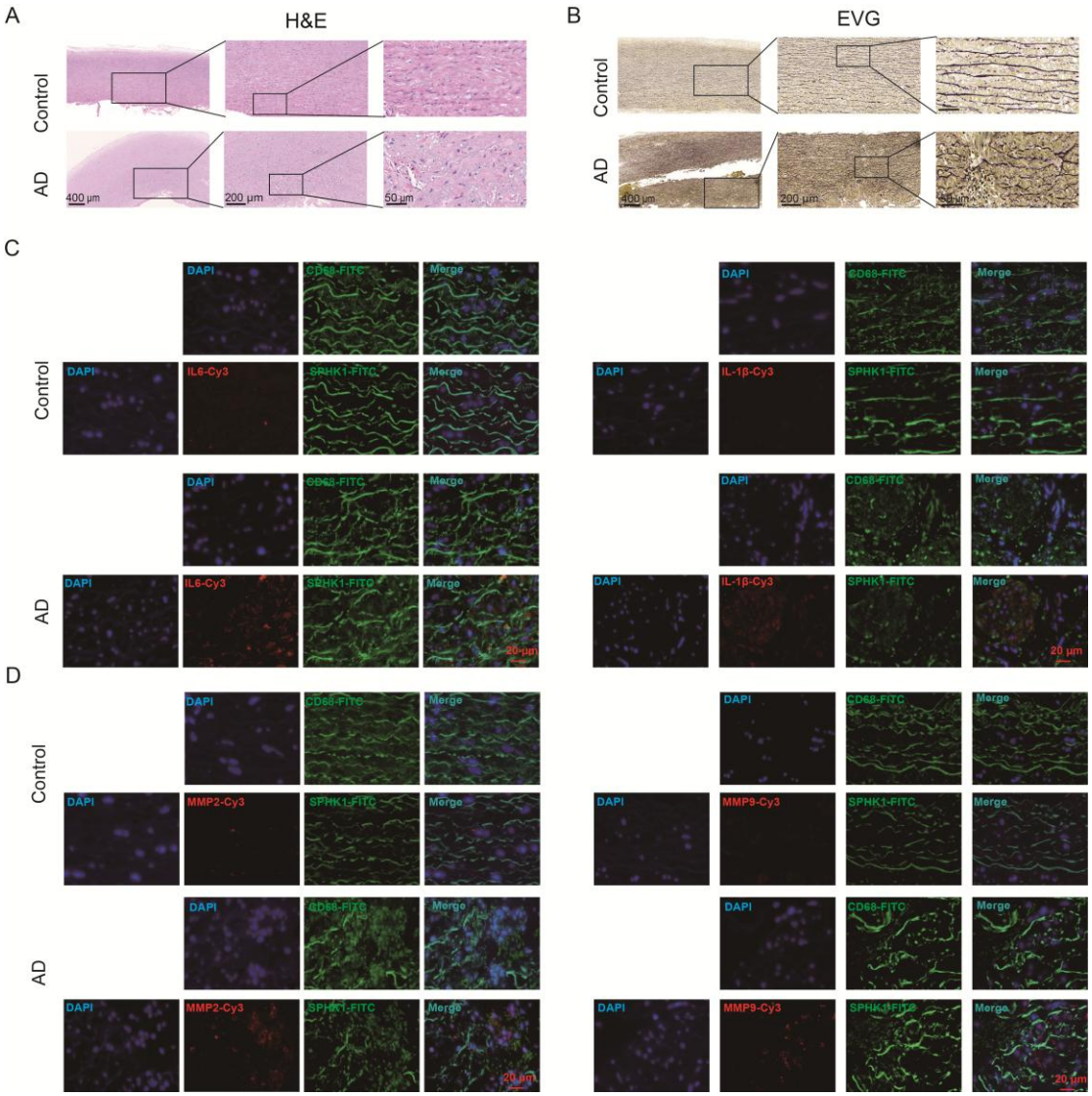

Figure S5. **Analysis of inflammatory injury in the aortic wall and the correlation between S1PRs and clinical case data. (A)** Representative H&E staining revealed the rupture, dissolution of blood clots, and infiltration of local immune cells in human aortic dissection. Scale bars: 400 μm, 200 μm, 50 μm. **(B)** Representative EvG staining revealed the rupture of elastic fibers in the aortic dissection. Scale bars: 400 μm, 200 μm, 50 μm. **(C)** Representative IF shown the expression levels of MMP2, MMP9 in $CD68^{+}SPHK1^{+}$ regions of aortic dissection and normal aorta tissues, scale bars are 20 μm (400×). **(D)** Representative IF shown the expression levels of IL-6, IL-1β in $CD68^{+}SPHK1^{+}$ regions of aortic dissection and normal aorta tissues, scale

bars are 20 μm (400×).

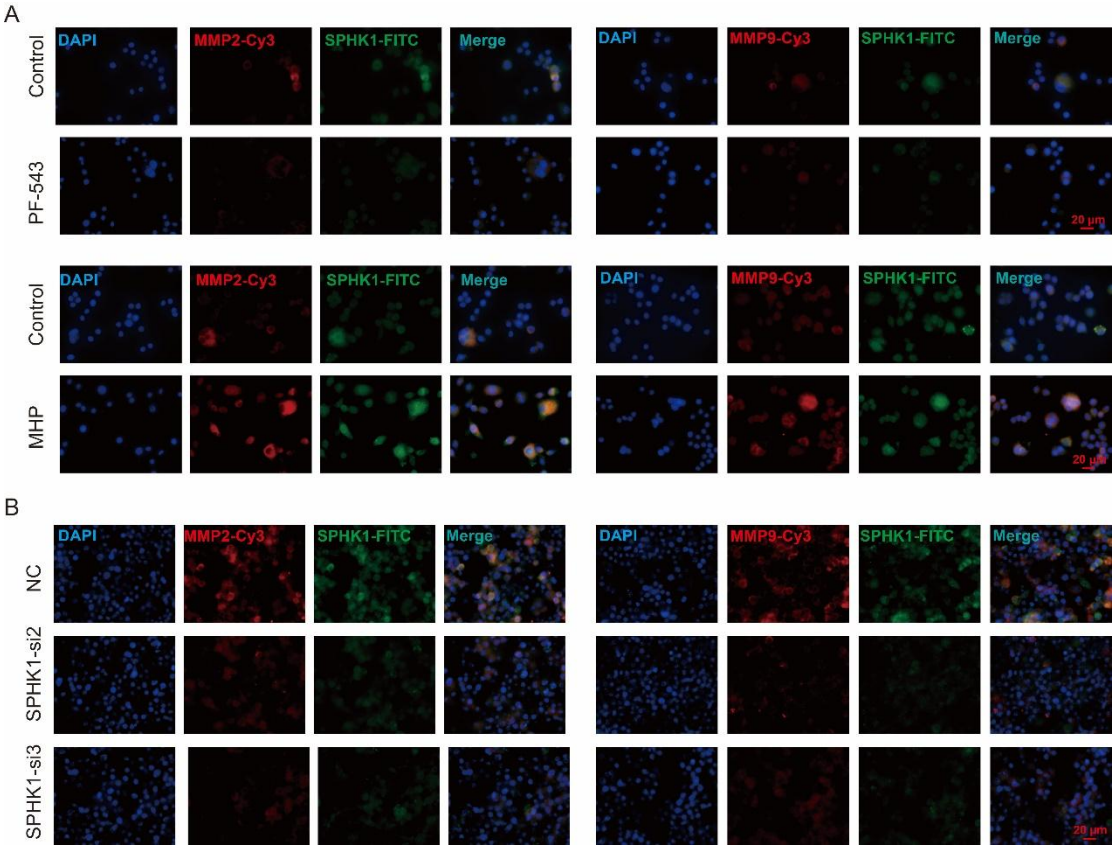

Figure S6. **Detection of inflammatory mediator expression following SPHK1 expression or functional intervention. (A)** Cell immunofluorescence showed that in PF-543-treated RAW264.7 cells, the co-expression of SPHK1 with MMP2 and MMP9 was reduced, conversely, in MHP-treated RAW264.7 cells, the co-expression of SPHK1 with MMP2 and MMP9 was enhanced. **(B)** Immunofluorescence co-localization studies demonstrated that SPHK1 knockdown resulted in reduced fluorescence signals of SPHK1 with MMP2 and SPHK1 with MMP9. A,B with a scale bar of 20 μm (400×).

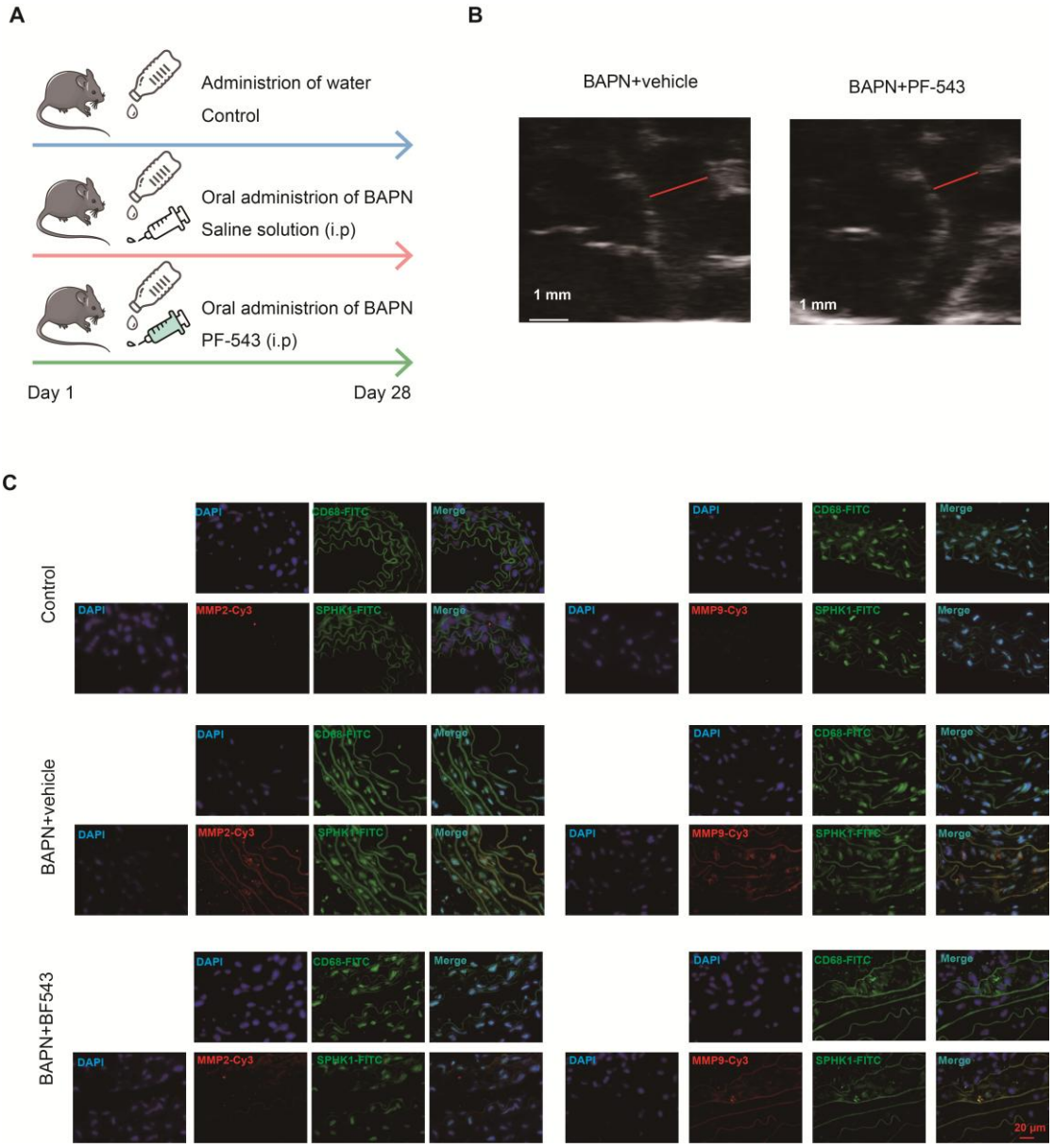

Figure S7. SPHK1 Inhibitor PF-543 Mitigates Aortic Dilation and inflammatory injury in AD Mice. (A) Schematic diagram of the drug treatment process for mice, with 20 mice per group, undergoing a 28-day treatment regimen. i.p. refers to intraperitoneal injection. **(B)** Representative ultrasonographic images of aortic dissection in mice. Scale bar, 1 mm. **(C)** Representative images of immunofluorescent staining of $CD68^{+}SPHK1^{+}$ regions and MMP2, MMP9 in mouse aortic tissues under different interventions, scale bar, 20 μm (400×).